Scientific Reports

https://doi.org/10.1038/s41598-026-42466-3

Article in Press

Development of Quantum dot-based enzyme biosensor for the detection of dopamine in urine

Received: 21 November 2025

Accepted: 25 February 2026

Published online: 12 March 2026

Cite this article as: Yogaraju D.S., Shetty N.S., Mohideen S. *et al.* Development of Quantum dot-based enzyme biosensor for the detection of dopamine in urine. *Sci Rep* (2026). https://doi.org/10.1038/s41598-026-42466-3

Dhaarini Sakharayapatna Yogaraju, Nidhi S. Shetty, Suhana Mohideen, Shama Prakash K & Akshath Uchangi Satyaprasad

Development of Quantum dot-based enzyme biosensor for the detection of dopamine in urine

Dhaarini Sakharayapatna Yogaraju[1], Nidhi S Shetty[1], Suhana Mohideen[$], Shama K Prakash[&], Akshath Uchangi Satyaprasad[$*]

Author affiliations

[1]Equal contributions

[1$] Nitte (Deemed to be University), Nitte University Centre for Science Education and Research-NUCSER, Department of Bio and Nanotechnology, Mangalore, Karnataka, India.
[1$] Nitte (Deemed to be University), Department of Biochemistry, K. S Hegde Medical Academy (KSHEMA), Mangalore, Karnataka, India.

[&] Nitte (Deemed to be University), Department of General Medicine, K S Hegde Medical Academy, Mangalore, Karnataka, India.

*Correspondence to:

Dr. Akshath U. S, Marie-Curie Fellow,
Scientist GII, Department of Bio & Nanotechnology,
Nitte University Centre for Science Education and Research-NUCSER,
Department of Biochemistry, K. S Hegde Medical Academy (KSHEMA)
Nitte (Deemed to be University), Paneer Campus,
Kotekar-Beeri Road, Deralakatte Mangalore, Karnataka, India-575018,
akshath.uchangi@nitte.edu.in

akshathuchangi@gmail.com

Abstract

Dopamine (DA), a neurotransmitter released by the hypothalamus, plays a significant role in maintaining mental well-being. Abnormal DA level leads to neurological disorders such as depression and schizophrenia. Consequently, DA is commonly monitored in urine using various analytical methods as a non-invasive approach for assessing its physiological status. The available methods for DA detection are laborious and time-consuming. To circumvent this issue, we developed a Quantum dot-based enzyme biosensor for the rapid, sensitive detection of DA. Fluorescence quenching of QDs was in proportion with the DA concentration and was found to be linear with an $R^2 = 0.99$, with $p < 0.05$. The biosensor used to detect DA in urine samples in the range of 1.2 µM-8 µM, with $R^2 = 0.97$ and $p < 0.05$, and a limit of detection (LOD) of 1.2 µM in a urine sample (1:100). Spiking and recovery analysis in urine showed 94-98 % recovery with $p < 0.05$. The developed method showed specificity towards detecting DA in the presence of common interfering factors such as uric acid and ascorbic acid. The results show that dopamine-specific quenching is consistent and concentration-dependent, effectively distinguishing the target from background components in complex samples. This approach provides a promising platform for reliable DA monitoring in clinical diagnostics.

Keywords: Dopamine detection, Quantum dots, Enzyme biosensors, Fluorescence quenching

Abbreviations: Dopamine (DA), Tyrosine hydroxylase(TH), Gold nanoparticles (AuNPs), Glutathione(GSH), Gold nanoclusters(AuNCs), Quantum Dots (QDs), High performance liquid chromatography (HPLC), Enzyme-linked immune sorbent assay (ELISA), Cadmium Telluride(CdTe), fluorescence resonance energy transfer (FRET), Nitrogen doped -Graphene oxide quantum dots (N-GOQDs), Horseradish peroxidase (HRP), Uric acid (UA), Ascorbic acid (AA), Surface of glassy electrode (GCE)

Introduction:

Dopamine (DA), [4-(2-aminoethyl) benzene-1,2-diol], a neurotransmitter and a "feel-good hormone," is synthesized primarily in the brain in the ventral tegmental area, substantia nigra, and hypothalamus[1]. It plays a significant role in the central nervous system, and abnormal levels of DA can lead to some vital neurological diseases like schizophrenia, Parkinson's disease, and depression[2]. DA synthesis occurs via a two-step enzymatic reaction in which L-Tyrosine is converted to L-DOPA by tyrosine hydroxylase (TH). A further decarboxylation reaction catalyzed by DOPA decarboxylases produces DA[1]. The enzyme TH regulates DA biosynthesis, as well as that of other catecholamines. Hence, it is a promising approach for gene therapy and related treatment modalities[1]. Considering an average of 2 L of urine produced per day, it corresponds to 0.2-0.4 µmol/L[3]. In addition to these biological fluids, DA levels were monitored non-invasively in tear fluid. Schirmer's strips and capillary tubes are utilized to extract tears and measure DA levels[4]. Recent studies and techniques used to detect DA include conventional liquid chromatography[5], electrochemical detection coupled with high-performance liquid chromatography (HPLC)[6], microdialysis with capillary liquid chromatography[7], colorimetric[8,9], enzyme-based methods[10], enzyme-linked immunosorbent assay (ELISA)[11], etc. Due to the presence of DA at lower concentrations in body fluids, a highly sensitive detection method is often required. Long chromatographic run times, lack of specificity in the colorimetric method for detecting structurally similar catecholamines, cross-reactivity, enzyme instability, the need for skilled personnel, and the requirement for advanced instrumentation make the currently available techniques less reliable and efficient. Hence, biosensors developed using fluorescent tags or nanomaterials, which address the limitations of conventional methods, can improve the robustness, specificity, and sensitivity of detection[12,13,14].

The low detection limit and reliability of fluorescent techniques [15] have recently brought them to prominence. The fluorescent signals emitted by nanomaterials, such as surface-coated Quantum Dots (QDs) that are functionalized with biomolecules, such as enzymes,

make them useful as biosensors[16]. Quantum dots, such as nitrogen-doped carbon dots (N-GQDs), are used for sensitive detection of DA in human urine and serum samples via fluorescence quenching, with an acceptable accuracy of >80 % and a detection limit of up to 4 nM[17]. A recent study using graphene quantum dots (GQDs) established a label-free fluorescence approach for sensitive DA detection. The addition of DA quenched the early blue fluorescence due to photoinduced electron transfer from boron sulfur co-doped QDs to DA-quinone. The fluorescence quenching of GQDs was linearly proportional to the increasing concentration of DA[18]. Also, GQD surfaces conjugated with polypyrrole enable sensitive detection of DA with a detection limit of 10 pM, where the interaction between polypyrrole's amine group and DA's hydroxyl group leads to a strong enhancement in fluorescence intensity[19]. An electrochemical biosensor, which is a novel imprinted polymer fabricated with NiS_2 (Nickel disulfide) coated onto gold nanoparticles (AuNPs) and nitrogen-doped Graphene oxide quantum dots (N-GOQDs), is used for the sensitive and selective determination of DA in the nanomolar range with 93.9-106.15 % recovery rate in human urine, serum, and pharmaceutical samples[20]. In another study, Glutathione (GSH) protected gold nanoclusters (AuNCs) were used as fluorescent probes to detect DA. DA was oxidized to quinone in the presence of tyrosinase, which quenched the initial fluorescence of the AuNCs. In the presence of fluorescence intensity variation, a selective sensing assay was developed to detect DA with a LOD of 1 nM[21]. Polymer coating onto the surface of CdTe QDs exhibited considerable upconversion luminescence with two-photon excitation that aids in electron transfer from quinone to DA, which in turn was induced by DA anchored onto the surface of QD, leading to upconversion luminescence QD quenching. This method was able to detect DA down to a lower limit of 5.4 nM in biological fluids [22]. The work could not only provide insights into Tyrosinase and DA activity but also unlock potential strategies for tyrosinase inhibitor studies. However, the lack of evaluation using biological samples limits the practical applicability of these methods, as the matrix components could pose a challenge during detection. There are a few reports on electrochemical-based CdTe QD carbon electrodes for DA detection in urine[23], QDs embedded in imprinted polymers[24], and HRP-based systems for phenolic compounds[25], with a focus mainly on H_2O_2-mediated quenching rather than DA as the primary analyte. To the best of our knowledge, the present work is the first fluorescence biosensing platform validated in the urine matrix. With this background, we have developed a Cadmium Telluride (CdTe) quantum dot-based enzyme biosensor to detect DA in the current study, as they have tunable emission across the visible spectrum such as broad absorption spectra and narrow emission spectra, highly sensitivity to different quenchers, enable water solubility, the presence of thiol group in mercaptopropionic acid in the cap facilitate surface functionalization of different ligands and offer good photostability that is

resistant to photobleaching than other QDs[26].In the presence of Horseradish peroxidase (HRP) and H_2O_2 as a substrate, DA oxidizes to its quinone form. This results in fluorescence quenching due to the interaction of the quinone form of DA and the CdTe QDs. Electron acceptance of quinone by the excited state of QDs/electron transfer mechanisms like fluorescence resonance energy transfer (FRET)[27] or adsorption of quinone molecules on the QD surface[28] may alter their electron emission pattern and photoluminescent properties, thereby causing quenching. Using FRET, the quenching mechanism in which DA-quinone serves as the acceptor and CdTe QDs as energy donors is studied through non-radiative energy transfer. The interaction produces quinone species, which act as "dark quenchers" by accepting electrons or energy from QDs and decreasing their fluorescence. This non-radiative energy-transfer technique has been well established in our earlier report[29]. Based on this, the present study was conducted, in which the proposed method is a sensitive fluorescence-based method for detecting DA in a urine sample by quenching the fluorescence of CdTe QDs catalyzed by HRP[30]. In addition to establishing a reliable and sensitive platform for DA detection, the method is also validated by demonstrating practical applicability and efficacy in urine samples, showcasing its potential in diagnostics. DA detection using CdTe QDs that was doped on the surface of glassy electrode (GCE) - CdTe QDs/GCE showed an LOD of 300 nM, where there is no usage of enzyme and H_2O_2 in the presence of interferents such as uric acid (UA), glucose and ascorbic acid(AA)[31], also the detection by molecular imprinted electrode (MIP) for DA detection exhibited selectivity against UA, AA and tyramine as interferents with an LOD of 650 nM[32]. While many existing sensing platforms exhibit high sensitivity, they are often susceptible to cross-reactivity because they lack biorecognition elements. The current method utilizes enzymes to ensure the necessary specificity for accurate detection in complex biological samples.

2. Materials and methods

2.1 Chemicals and reagents

All reagents were of analytical grade and used as received without further purification. Cadmium telluride Quantum Dots (CdTe QDs), core type QDs (λ_{em} 610 nm), Dopamine hydrochloride, and HRP were purchased from Sigma Aldrich, USA. Sodium phosphate dibasic heptahydrate and Sodium phosphate monobasic monohydrate for phosphate buffer (PB) preparation, and Hydrogen peroxide (H_2O_2) were purchased from Sigma Aldrich, USA. Urine samples for the study were collected from healthy volunteers after obtaining the necessary ethical clearance. Water used for reagent preparations was collected from the Millipore ultrapure system (Type 1). The data were collected using a Spectrofluorimeter (FP-8300, Jasco, Japan) for photoluminescence measurements.

2.2 Enzyme assay

2.2.1 Optimization of Enzyme Concentration

To optimize HRP concentration, CdTe QDs (1 mg/mL) and DA (5 µM) were incubated for 5 min, followed by the addition of 300 µM H_2O_2 as a substrate. A varying concentration of HRP 2 U-12 U was prepared using phosphate buffer (1 mM PB, pH 7.4). In alkaline conditions, DA undergoes faster chemical autoxidation; however, pH 7.4 was chosen to maintain the structural integrity and optimize the efficiency of the HRP enzyme, which performs best at physiological levels. This setup ensures that the detected signal arises from enzymatic activity rather than non-specific base-catalyzed oxidation, thereby improving the assay's selectivity and accuracy. The enzyme was added to the reaction mixture and incubated for 10 min at 37 ºC. The Fluorescence spectra were recorded by exciting QDs (λ_{ex} 410 nm).

2.2.2 Optimization of H_2O_2 concentration

Optimized concentrations of QDs (CdTe QDs-1 mg/mL) were incubated with DA, followed by the addition of various concentrations of H_2O_2 (0.01 µM to 300 µM). All experiments were performed in triplicate (n=3). In a separate experiment, CdTe QDs were incubated with various concentrations of H_2O_2 (10 nM-300 µM) to evaluate fluorescence quenching at a fixed concentration of the enzyme (6 U) and DA (5 µM), and fluorescence quenching was monitored for 10 min. H_2O_2 kinetics experiments were performed in triplicate (n=3).

2.3 Dopamine detection

DA at varying concentrations (1.2 µM- 4 µM) was prepared in PB, and the enzyme assay was performed using optimized enzyme and substrate concentrations. All experiments were performed in triplicate (n=3). The reaction mixture was incubated for 10 min, and the fluorescence spectra were recorded.

2.3.1 Dopamine detection in Urine samples

After obtaining ethical clearance from the central ethics committee (INST.EC/2023-24/001), DA detection was performed on urine samples. The interaction of urine samples with the proposed biosensing system was first evaluated. The urine samples were diluted (1:100 PB) to reduce the matrix effects. The urine samples were incubated with an optimized concentration of QDs, enzyme, and substrate, and fluorescence quenching was evaluated for 10 min (without DA). Further, DA at various concentrations (1.2 µM- 8 µM) was prepared and spiked into urine samples. As discussed earlier, the enzymatic assay was performed, and fluorescence spectra were recorded.

2.3.2 Spiking and recovery studies

Urine samples were collected from the donor and spiked with various DA concentrations (1.2 µM-8 µM), and the assay was performed as discussed in section 2.3.1. The recovery percentage was calculated as provided in Table 1; all experiments were performed in triplicate (n=3).

2.4. Interference of uric acid, ascorbic acid, and different organic and inorganic constituents in urine in the detection of DA

The interference of uric acid and ascorbic acid at physiological normal concentrations was chosen to assess their impact on DA detection in urine samples. The urine samples were diluted (1:100 PB) to reduce the matrix effects. Uric acid kinetics were performed in triplicate with the concentrations ranging from 160 µM, 321 µM, and 441 µM, which were spiked to the urine sample with an optimized concentration of QDs, (6 U) enzyme, (300 µM) substrate, and fluorescence quenching, which was evaluated for 10 min (without DA), and fluorescence spectra were recorded. Similarly, ascorbic acid kinetics was performed at 283 µM, 425 µM, and 567 µM in triplicate. Interference of uric acid in the detection of DA was checked by spiking DA at 1.2 µM, 4 µM, and 8 µM to three different concentrations of uric acid, with respect to a control where no DA was spiked to uric acid. Followed by checking the interference of various organic (glucose) and inorganic constituents (sodium, sulfate, phosphate, potassium) present in the urine sample.

3. Results and discussion

3.1 Optimization of enzyme concentration

HRP, an oxidoreductase, catalyzes the oxidation of DA in the presence of H_2O_2[33]. To optimize the enzyme concentration required for the oxidation of DA to dopaquinone in the presence of H_2O_2, an enzyme kinetic assay was performed. As depicted in Fig. 1a, an increasing concentration of HRP from 6 U to 12 U resulted in a progressive reduction in relative fluorescence intensity. The quenching fluorescence ratio (F/Fo) of CdTe QDs was in proportion to the HRP concentrations (F/Fo 1.35-0.90, HRP 6 U-12 U). A maximum fold decrease in fluorescence (F/Fo=0.88) was observed at 6 U, and further changes were not significant. Based on these results, since maximum fluorescence quenching is observed at 6 U HRP concentration, which is fixed for the rest of the study, suggesting the enzyme has reached its maximal catalytic turnover rate under fixed substrate concentration (300 µM), consistent with Michaelis-Menten saturation behavior[34]. The spectral trend indicates that 6U HRP was sufficient for near-complete oxidation of 5 µM DA under the set experimental conditions. A kinetic profile similar to this was observed in a study in which phenol was oxidized by HRP, following an irreversible Michaelis-Menten reaction in the presence of H_2O_2, thereby identifying the rate-limiting step[35]. This aligns with the observation that reaction rates increase with substrate concentration but level off once the enzyme is

saturated. There will be a substantial shift in the reaction rate, as observed in the kinetics curve, after the rate reaches its saturation point[36], leading to the oxidation of DA to quinone. DA oxidation to quinone is observed by fluorescence quenching of CdTe QDs, which increases with increasing incubation time[37]. CdTe QDs were used at a working concentration corresponding to the 1 mg/mL stock per reaction, which was empirically found to provide sufficiently high fluorescence intensity without detector saturation, and to allow clear observation of DA-induced quenching.

3.2 Optimization of H_2O_2 concentration and H_2O_2 interference

H_2O_2 is a common oxidant produced by oxidases. Its unstable bonds lead to breakdown, forming hydroxyl ions or radicals used in sensing. Reaction conditions influence the formation of hydrogen and oxygen. Active sites in the sensor catalyze the formation of OH• radicals, driving H_2O_2 degradation [38],[39]. H_2O_2 breakdown releases electrons that are used in the conversion of DA to Quinone, serving as a substrate utilized in the present study, analyzed by fluorescence quenching of CdTe QDs. O_2(aq)/H_2O_2 and DQ/DdxQH_2 (catechol/quinone moiety) redox potentials show that the two-electron oxidation of DA by the oxygen/hydrogen peroxide redox pair is thermodynamically advantageous at all pH values[40]. Fluorescence quenching of CdTe QDs for the breakdown of the substrate H_2O_2 is observed in the ratio (F/Fo), which was in alliance with the lowest (0.01 µM) to the highest concentration of H_2O_2 (300 µM). The fluorescence quenching ratio (F/Fo =0.19) for the highest concentration of H_2O_2 (300 µM) and (F/Fo= 0.98) was for the lowest (0.01 µM) H_2O_2. It is important to note that the highest concentration of H_2O_2 (300 µM) significantly reduces the intensity, showing a threshold effect (Fig. 1b). Fig. 1b shows a control with QD, H_2O_2, and HRP without DA; Fig. 1c shows a control with QD in PB. At 0.01 µM concentration of H_2O_2, fluorescence quenching ratio (F/Fo) for 0.01 µM H_2O_2 concentration was 0.98 in comparison to the highest concentration (300 µM) (F/Fo=0.195), suggesting that a low concentration of H_2O_2 maintains intensity, having a very minimal effect on the intensity of the reaction. The highest H_2O_2 concentration shows a greater effect in the presence of 6 U of HRP enzyme concentration, CdTe QDs, and 5 µM DA concentration, all dissolved in PB of pH 7.4. Among the concentrations ranging from 0.01 µM-300 µM of H_2O_2 tried in the presence of HRP enzyme and DA, there is only a minimal effect observed at 0.01 µM H_2O_2 concentration and a maximum effect observed at 300 µM H_2O_2. Based on these results, 300 µM H_2O_2 was determined to be the optimal concentration for the reaction. In the absence of HRP and DA in the reaction mixture, there is little effect on the fluorescence quenching of H_2O_2 kinetics, as shown in Fig. 2b. The kinetics was carried out only in PB and QD with varying concentrations of H_2O_2, fluorescence quenching ratio (F/Fo=1.055) for 300 µM H_2O_2.

This states that, for fluorescence quenching to occur, the interaction of H_2O_2 with HRP (6 U) and DA (5 µM) is necessary [41,42].

3.3 Dopamine biosensing

After fixing the H_2O_2 concentration and reaction time, different DA concentrations (1.2 µM to 4 µM) dissolved in MilliQ water were tested. Oxidation of DA to quinone in the presence of H_2O_2 as a substrate occurs on the surface of the HRP enzyme, which is analyzed by fluorescence quenching of QDs[43-44]. The reaction mixture consists of 6 units of HRP, 300 µM H_2O_2, and different concentrations of DA in PB at pH 7.4, where concentration-dependent fluorescence quenching was observed, excited at λ_{ex} 420 nm. The highest concentration of DA (4 µM) showed a fluorescence quenching ratio (F/Fo=0.137) with respect to the control intensity, and a (F/Fo=0.92) fluorescence quenching ratio for 1.2 µM of DA compared with the control was observed after 10 minutes of incubating all the reaction components (Fig.2a). Fig 2 consists of controls with QD, H_2O_2, and HRP with no DA. Oxidation of DA to quinone is due to the presence of H_2O_2, which releases electrons that are utilized in the oxidation step in the presence of HRP as an enzyme[30]. This HRP-based QD biosensor had a detection limit of 1.2 µM and showed activity with a linear range of 1.2 µM to 4 µM[45]. The relationship between fluorescence intensity and DA concentration was plotted as a standard deviation graph with (R^2 = 0.99) (Fig. 2b), indicating that the developed method is sensitive and reliable. Also, one-way ANOVA was performed, which showed a $p<0.0001$ from 1.8-4 µM, showing statistical significance (Fig. 2c).

3.4. Different dilutions of urine in Dopamine biosensing

In order to investigate the interference of urine components in DA biosensing through matrix effect, urine sample from a healthy individual was diluted in PB buffer at various ratios where 1 part is urine sample diluted in 19 parts of PB v/v, including 1:20, 1:30, 1:40, 1:50, 1:100, 1:150, and 1:200. The interference of components of urine was checked in the reaction mixture with control's having the enzyme (HRP) and substrate (H_2O_2) without DA. Fig.3a depicts the spectra of different urine dilutions having QD in PB as a control, and Fig.3b depicts the spectra of different urine dilutions having only H_2O_2 along with QD in PB as a control. At 1:20-1:50, we observed a clear reduction in fluorescence upon treatment with the reaction mixture, which could be attributed to the urine matrix. To reduce non-specific signals, we used a 1:100 dilution factor and did not further dilute the urine sample.

3.5. Dopamine biosensing in Urine samples

The fluorescence quenching of DA was evaluated in DA-spiked urine samples using a quantum dot–enzyme-based biosensor system. Fig. 4a shows a systematic decrease in

relative fluorescence intensity with increasing DA concentration from 1.2 µM to 8 µM under reaction conditions similar to those in the aqueous system. Fold decrease(F/Fo) was used to quantify the degree of quenching. Compared with the control, F/Fo values declined progressively from 0.90 at 1.2 µM to 0.18 at 8 µM. The kinetic behavior is consistent with previous results on the detection of DA in aqueous systems, validating that the biosensing platform retains its functionality even in complex matrices. A recovery study was conducted using urine samples spiked with varying DA concentrations (1.2 µM-7.2 µM), showing % recovery ranging from 94.25 % to 98.62 %, emphasizing the analytical accuracy and minimal matrix-induced suppression effects (Table 1). The level of recovery is consistent with prior reports with fluorescent nanoparticle-based biosensors for DA detection in biological fluids[46,47,48]. The linear standard curve (R^2 = 0.97877) with a strong negative correlation (Pearson's r = -0.98933) between relative fluorescence intensity and DA concentration (Fig. 4b) indicates the reliability and sensitivity of the developed biosensor, which can be further extended to multiplexed detection in other body fluids. Detection of DA in spiked urine samples was compared with that of control at 4 µM and 8 µM (Fig.4c). While Fig.5a explains the spike and recovery of DA in the urine sample, which is analyzed using one-way ANOVA. As DA exists as a free base in biological fluids such as urine, 65-400 µg/24 h (0.42–2.61 µM for 1 L urine), which was studied in a healthy population, where 521.7 µg/24 h (3.4 µM) is the highest DA concentration due to dietary intake and the subject being studied[49]. To ensure clinical relevance, the sensor's analytical performance was validated in a real human urine matrix, accounting for potential matrix effects absent in aqueous standards. The testing range was extended to 8.0 µM to encompass the full clinical spectrum, bridging the gap between the healthy physiological maximum ~3.4 µM[49] and pathological hyper-excretion levels observed in conditions such as metastatic paraganglioma, which can reach 3187.5 µg/day (~20.8 µM)[50]. The linear quantification range is optimized to 4.0 µM in aqueous samples; however, the sensor remains highly effective for detecting pathological hyperexcretion of DA up to 8.0 µM.

3.6. Interference of uric acid, ascorbic acid, and different organic and inorganic constituents in urine in the detection of DA

The standard graph and recovery studies for DA detection were performed on the urine sample to avoid interference from commonly occurring urine components. As depicted in Fig. 5b, ~50 % fluorescence quenching was observed with the QD+urine+enzyme system, which can be attributed to HRP-mediated oxidation of interfering molecules. The control was normalized, and varying DA concentrations were added, and the biosensor response was evaluated. Nevertheless, to show biosensor robustness, we spiked various organic and inorganic constituents into the urine sample (1:100), and the fluorescence quenching pattern

was evaluated. We observed that uric acid (UA of 160-441 µM) can quench fluorescence (Fig.6a)[51]. It is important to note that uric acid alone showed 10-15 % quenching of the fluorescence, nevertheless, upon addition of 1.2 µM/ 8 µM of DA the quenching was further increased in response to enzyme reaction to ~25-56 % showing the robustness of biosensor (Fig.6b). Additionally, the broad-spectrum interference study involving major electrolytes (Na^+, K^+, SO_4^{2-}, PO_4^{3-}) and metabolites (glucose, creatinine) showed a negligible interference (Fig.5b).

4. Conclusion

The CdTe QD-based fluorescence biosensor provides an effective and sensitive platform for detecting DA. Systematic standardization of substrate, enzyme, and reaction time revealed that 300 µM H_2O_2, 6 U HRP, and 10 minutes of incubation are optimal for maximal quenching of fluorescence and subsequent DA detection via oxidation of DA to dopaquinone. The real-world applicability of the biosensor was validated using DA-spiked urine samples, which showed a remarkable detection response from 1.2 µM to 8 µM of DA, with recovery percentages ranging from 94.25 % to 98.62 %. A strong correlation between different DA levels and relative fluorescence intensity underscores the nanosensor's reliability and potential, paving the way for multiplexed biosensing in other biological fluids.

Author contributions

D.S.Y. and N.S.S: Methodology, investigation, data curation, visualization, graphic design, manuscript writing – original draft, review, and editing. S. M.; Methodology and investigation, S. K. P.: CEC and sample collection. A. U. S.: Conceptualization, visualization, supervision, writing, manuscript review and critical evaluation, and final approval of the version to be published.

Data availability statement

All data generated or analysed during this study are included in this article.

Conflicts of interest

The authors declare that they have no known competing financial interests or personal relationships that could have appeared to influence the work reported in the paper.

Funding

This work was funded by Nitte (Deemed to be University) Grant Number-N/RG/NUFR1/NUCSER/2021/01, Nitte University Centre for Science Education and Research (NUCSER), Mangaluru, India.

Acknowledgements

The authors acknowledge the support and facilities provided by Nitte (Deemed to be University).

References:

1. Juárez Olguín, H., Calderón Guzmán, D., Hernández García, E. & Barragán Mejía, G. The Role of Dopamine and Its Dysfunction as a Consequence of Oxidative Stress. *Oxid. Med. Cell. Longev.* **2016**, 9730467 (2016).

2. Chang, G.-Y., Kurniawan, D., Chang, Y.-J. & Chiang, W.-H. Microplasma-Enabled Surfaced-Functionalized Silicon Quantum Dots for Label-Free Detection of Dopamine. *ACS Omega* **7**, 223–229 (2021).

3. Beatto, T. G., Gomes, W. E., Etchegaray, A., Gupta, R., & Mendes, R. K. Dopamine levels determined in synthetic urine using an electrochemical tyrosinase biosensor based on ZnO@ Au core–shell. *RSC Adv.* **13**, 33424–33429 (2023).

4. Sharma, N. S. *et al.* Dopamine levels in human tear fluid. *Indian J. Ophthalmol.* **67**, 38–41 (2019).

5. Mochizuki, R. & Ogra, Y. Determination of intracellular dopamine by liquid chromatography–fluorescence detection with post-column derivatization using the König reaction. *Journal of Chromatography B* **1232**, 123956 (2024).

6. Zhou, Y. *et al.* Simultaneous analysis of dopamine and homovanillic acid by high-performance liquid chromatography with wall-jet/thin-layer electrochemical detection. *Analyst* **138**, 7246–7253 (2013).

7. Gu, H., Varner, E. L., Groskreutz, S. R., Michael, A. C., & Weber, S. G. In vivo monitoring of dopamine by microdialysis with 1 min temporal resolution using online capillary liquid chromatography with electrochemical detection. *Anal. Chem.* **87**, 6088–6094 (2015).

8. Liang, L., Zhao, Z., Ye, F., & Zhao, S. Rapid and sensitive colorimetric detection of dopamine based on the enhanced-oxidase mimicking activity of cerium (IV). *New Journal of Chemistry* **45**, 6780–6786 (2021).

9. Sun, Y., Peng, M., Wu, A. & Zhang, Y. Multicolor colorimetric detection of dopamine based on iodide-responsive copper–gold nanoparticles. *Chemical Communications* **59**, 12180–12183 (2023).

10. Jabbari, S., Dabirmanesh, B., Daneshjou, S. & Khajeh, K. The potential of a novel enzyme-based surface plasmon resonance biosensor for direct detection of dopamine. *Sci. Rep.* **14**, 14303 (2024).

11. Nichkova, M., Wynveen, P. M., Marc, D. T., Huisman, H. & Kellermann, G. H. Validation of an ELISA for urinary dopamine: applications in monitoring treatment of dopamine-related disorders. *J. Neurochem.* **125**, 724–735 (2013).

12. Sargazi, S. *et al.* Fluorescent-based nanosensors for selective detection of a wide range of biological macromolecules: A comprehensive review. *Int. J. Biol. Macromol.* **206**, 115–147 (2022).

13. Shetty, N. S., Othayoth, V. & Satyaprasad, A. U. Target-induced nanoparticle assemblies: a comprehensive review of strategies for nucleic acid functionalization{,} biosensing{,} and drug delivery applications. *Anal. Methods* **17**, 3876–3901 (2025).

14. Pramanik, R. Nanomaterial-enhanced fluorescence sensors for dopamine neurotransmitters: a photophysical perspective. *Analytical Methods* **17**, 4251–4292 (2025).

15. Zhao, J., Zhao, L., Lan, C. & Zhao, S. Graphene quantum dots as effective probes for label-free fluorescence detection of dopamine. *Sens. Actuators B Chem.* **223**, 246–251 (2016).

16. Ağbulut, M. S. B., Elibol, E., Çadırcı, M. & Demirci, T. Fluorescent CdTe/ZnS Core/Shell Quantum Dots for Sensitive Metabolite Detection in Real Samples. *J. Fluoresc.* 1–17 (2025).

17. Louleb, M. *et al.* Detection of dopamine in human fluids using N-doped carbon dots. *ACS Appl. Nano Mater.* **3**, 8004–8011 (2020).

18. Chatterjee, M. *et al.* Highly sensitive and selective detection of dopamine with boron and sulfur co-doped graphene quantum dots. *Sci. Rep.* **12**, 9061 (2022).

19. Zhou, X. *et al.* Dopamine fluorescent sensors based on polypyrrole/graphene quantum dots core/shell hybrids. *Biosens. Bioelectron.* **64**, 404–410 (2015).

20. Lu, Z. *et al.* A dual-template imprinted polymer electrochemical sensor based on AuNPs and nitrogen-doped graphene oxide quantum dots coated on NiS2/biomass carbon for simultaneous determination of dopamine and chlorpromazine. *Chemical Engineering Journal* **389**, 124417 (2020).

21. Teng, Y., Jia, X., Li, J., & Wang, E. Ratiometric fluorescence detection of tyrosinase activity and dopamine using thiolate-protected gold nanoclusters. *Anal. Chem.* **87**, 4897–4902 (2015).

22. Jin, H. *et al.* Two-photon excited quantum dots with compact surface coatings of polymer ligands used as an upconversion luminescent probe for dopamine detection in biological fluids. *Analyst* **140**, 2037–2043 (2015).

23. Yu, H. W., Zhang, Z., Jiang, J. H., Pan, H. Z., & Chang, D. Simple strategy for sensitive detection of dopamine using CdTe QDs modified glassy carbon electrode. *J. Clin. Lab. Anal.* **32**, e22320 (2017).

24. Khadem-Abbassi, K. *et al.* CdTe0.5S0.5/ZnS Quantum Dots Embedded in a Molecularly Imprinted Polymer for the Selective Optosensing of Dopamine. *Nanomaterials* **9**, 693 (2019).

25. Yuan, J., Guo, W. & Wang, E. Utilizing a CdTe Quantum Dots−Enzyme Hybrid System for the Determination of Both Phenolic Compounds and Hydrogen Peroxide. *Anal. Chem.* **80**, 1141–1145 (2008).

26. Nguqu, Z., Daramola, O. A. & Dejene, F. B. Effect of different cadmium sources on the optical and structural properties of CdTe quantum dots (QDs) co-stabilized with GSH-TGA. *Results Chem.* **15**, 102214 (2025).

27. Jiménez-López, J. *et al.* Exploiting the fluorescence resonance energy transfer (FRET) between CdTe quantum dots and Au nanoparticles for the determination of bioactive thiols. *Spectrochim. Acta A Mol. Biomol. Spectrosc.* **212**, 246–254 (2019).

28. Dwiecki, K., Neunert, G., Nogala-Kałucka, M. & Polewski, K. Fluorescence quenching studies on the interaction of catechin-quinone with CdTe quantum dots. Mechanism elucidation and feasibility studies. *Spectrochim. Acta A Mol. Biomol. Spectrosc.* **149**, 523–530 (2015).

29. Akshath, U. S., Shubha, L. R., Bhatt, P. & Thakur, M. S. Quantum dots as optical labels for ultrasensitive detection of polyphenols. *Biosens. Bioelectron.* **57**, 317–323 (2014).

30. Wang, H. Y., Feng, X. G., Zhang, M. & Zhao, H. Determination of dopamine in injections and urine by an enzyme-catalyzed fluorescence quenching method. *Anal. Sci.* **23**, 1297–1300 (2007).

31. Yu, H. W., Zhang, Z., Jiang, J. H., Pan, H. Z. & Chang, D. Simple strategy for sensitive detection of dopamine using CdTe QDs modified glassy carbon electrode. *J. Clin. Lab. Anal.* **32**, e22320 (2018).

32. Ciriello, R., Graziano, M., Bianco, G. & Guerrieri, A. Electrosynthesized Poly(o-aminophenol) Films as Biomimetic Coatings for Dopamine Detection on Pt Substrates. *Chemosensors 2021, Vol. 9,* **9**, (2021).

33. Yuan, J., Guo, W. & Wang, E. Utilizing a CdTe quantum dots− enzyme hybrid system for the determination of both phenolic compounds and hydrogen peroxide. *Anal. Chem.* **80**, 1141–1145 (2008).

34. Peletier, L. A. & Gabrielsson, J. Impact of enzyme turnover on the dynamics of the Michaelis–Menten model. *Math. Biosci.* **346**, 108795 (2022).

35. Vasudevan, P. T. & Li, L. O. Kinetics of phenol oxidation by peroxidase. *Appl. Biochem. Biotechnol.* **60**, 203–215 (1996).

36. Giaretta, J. E. *et al.* Flexible Sensors for Hydrogen Peroxide Detection: A Critical Review. *ACS Appl. Mater. Interfaces* **14**, 20491–20505 (2022).

37. Liu, J. *et al.* Recent progress in wearable near-sensor and in-sensor intelligent perception systems. *Sensors* **24**, 2180 (2024).

38. Salomäki, M., Marttila, L., Kivelä, H., Ouvinen, T. & Lukkari, J. Effects of pH and oxidants on the first steps of polydopamine formation: a thermodynamic approach. *J. Phys. Chem. B* **122**, 6314–6327 (2018).

39. Bhunia, S. K., Dolai, S., Sun, H. & Jelinek, R. “On/off/on” hydrogen-peroxide sensor with hemoglobin-functionalized carbon dots. *Sens. Actuators B Chem.* **270**, 223–230 (2018).

40. Ahmed, A. *et al.* Fluorescence-quenching-mediated detection of hydrogen peroxide using tungsten-incorporated graphitic carbon nitride nanoflakes. *RSC Adv.* **11**, 7479–7491 (2021).

41. Rendón, J. L. & Pardo, J. P. Time-Dependent Kinetic Complexities in Enzyme Assays: A Review. *Biomolecules* vol. 15 Preprint at https://doi.org/10.3390/biom15050641 (2025).

42. Huang, H. *et al.* Determination of catecholamine in human serum by a fluorescent quenching method based on a water-soluble fluorescent conjugated polymer–enzyme hybrid system. *Analyst* **137**, 1481–1486 (2012).

43. Stewart, A. J., Hendry, J. & Dennany, L. Whole blood electrochemiluminescent detection of dopamine. *Anal. Chem.* **87**, 11847–11853 (2015).

44. DeVoe, E. & Andreescu, S. Catalytic electrochemical biosensors for dopamine: design, performance, and healthcare applications. *ECS Sensors Plus* **3**, 20601 (2024).

45. Liu, X. & Liu, J. Biosensors and sensors for dopamine detection. *View* **2**, 20200102 (2021).

46. He, Y.-S. *et al.* Highly sensitive and selective dual-emission ratiometric fluorescence detection of dopamine based on carbon dots-gold nanoclusters hybrid. *Sens. Actuators B Chem.* **265**, 371–377 (2018).

47. Wu, H.-P., Cheng, T.-L. & Tseng, W.-L. Phosphate-modified TiO2 nanoparticles for selective detection of dopamine, levodopa, adrenaline, and catechol based on fluorescence quenching. *Langmuir* **23**, 7880–7885 (2007).

48. Zhao, Y., Yang, F., Zhao, L. & Xu, G. A Simple and Rapid Fluorescent Sensor Based on MoS2 Quantum Dots for Dopamine Detection. *J. Fluoresc.* https://doi.org/10.1007/s10895-025-04413-9 (2025) doi:10.1007/s10895-025-04413-9.

49. Basolo, A., Hollstein, T., Walter, M., Krakoff, J. & Piaggi, P. Urinary Dopamine Excretion Rate Decreases during Acute Dietary Protein Deprivation and Is Associated with Increased Plasma Pancreatic Polypeptide Concentration. *Nutrients 2021, Vol. 13,* **13**, (2021).

50. Takenaka, J. *et al.* Urinary Dopamine Levels Can Predict the Avidity of Post-Therapy [131I]MIBG Scintigraphy in Unresectable or Metastatic Pheochromocytomas and Paragangliomas: A Preliminary Clinical Study. *Pharmaceuticals 2025, Vol. 18,* **18**, (2025).

51. Pundir, C. S. Chapter 6 - Applications of Enzyme Nanoparticles. in *Enzyme Nanoparticles* (ed. Pundir, C. S.) 43–60 (William Andrew Publishing, Boston, 2015). doi:https://doi.org/10.1016/B978-0-323-38913-6.00006-4.

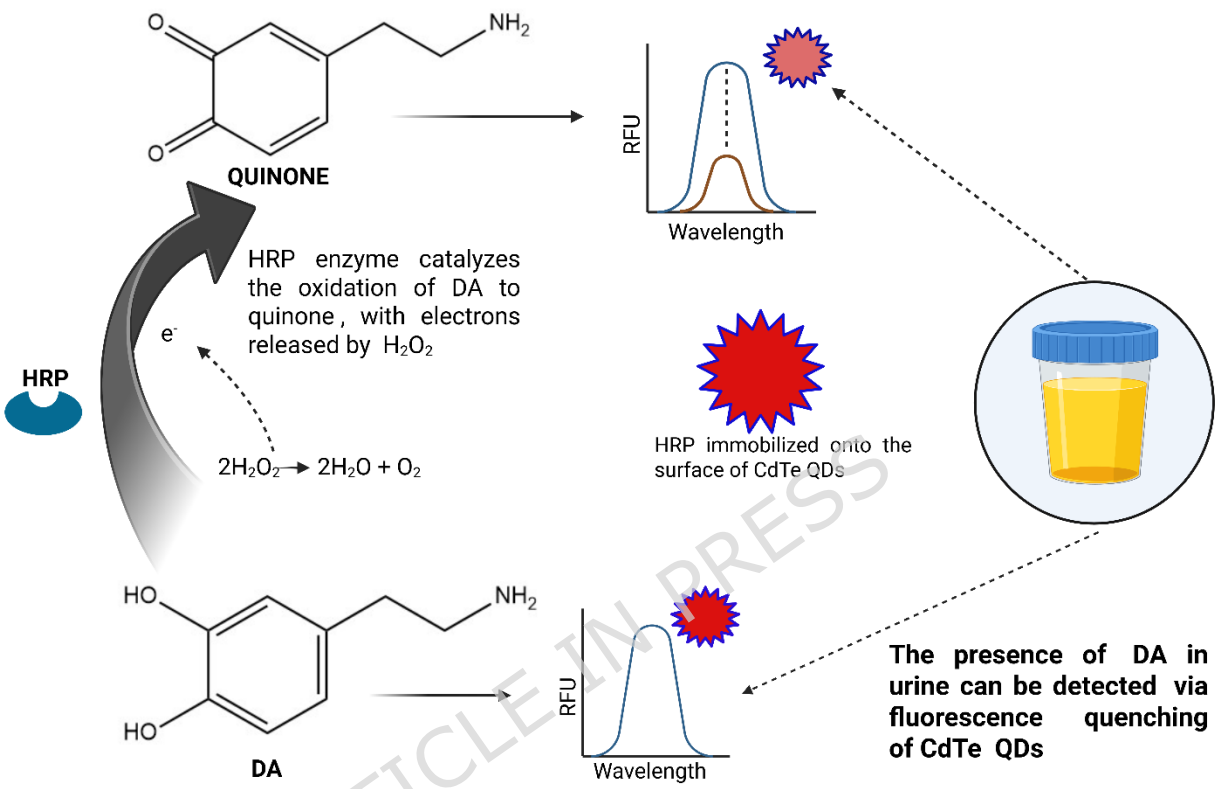

Scheme 1: Scheme showing the conversion of DA to Quinone by HRP immobilized on CdTe QDs.

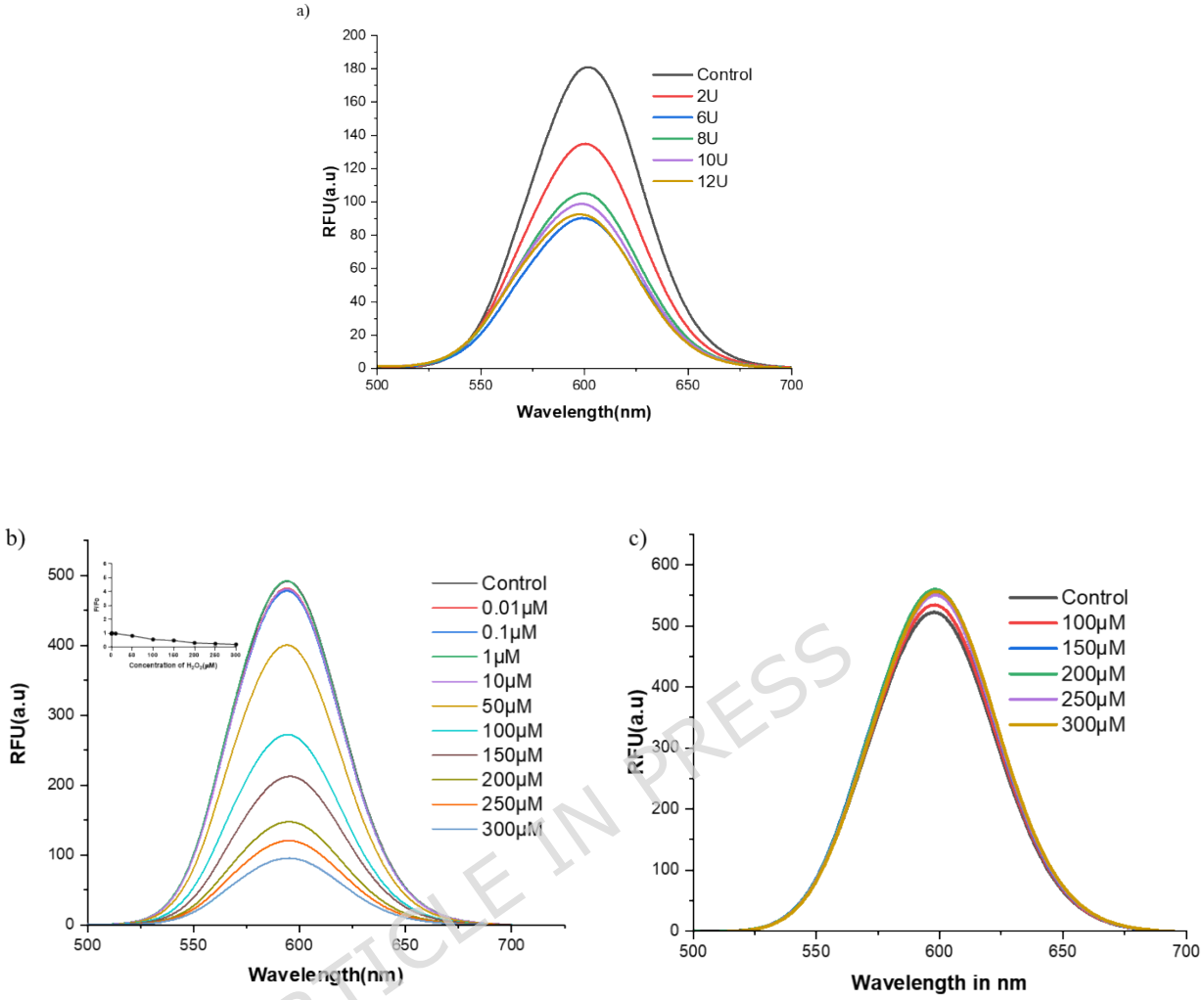

Fig.1: Enzyme Kinetics, H_2O_2 kinetics, and H_2O_2 interference spectra

a) Fluorescence emission spectra of CdTe QDs in the presence of varying concentrations of HRP, from 6 U to 12 U, at a fixed DA (5 μM) and H_2O_2 concentration (300 μM). Control represents QD, H_2O_2, and HRP with no DA in PB. Increasing the concentration of HRP results in enhanced fluorescence quenching until the enzyme reaches its saturation.

b) Fluorescence emission spectra of CdTe QDs in the presence of varying concentrations of H_2O_2 substrate, from 0.01 μM to 300 μM, at fixed DA (5 μM) and HRP (6 U). Control represents QD, H_2O_2, and HRP with no DA in PB. Increasing the concentration of H_2O_2 results in enhanced fluorescence quenching until it reaches saturation.

c) H_2O_2 interference with the fluorescence intensity of CdTe QDs in the presence of varying concentrations of H_2O_2 substrate only, from 0.01 μM to 300 μM, in the absence of enzyme and substrate with respect to the control.

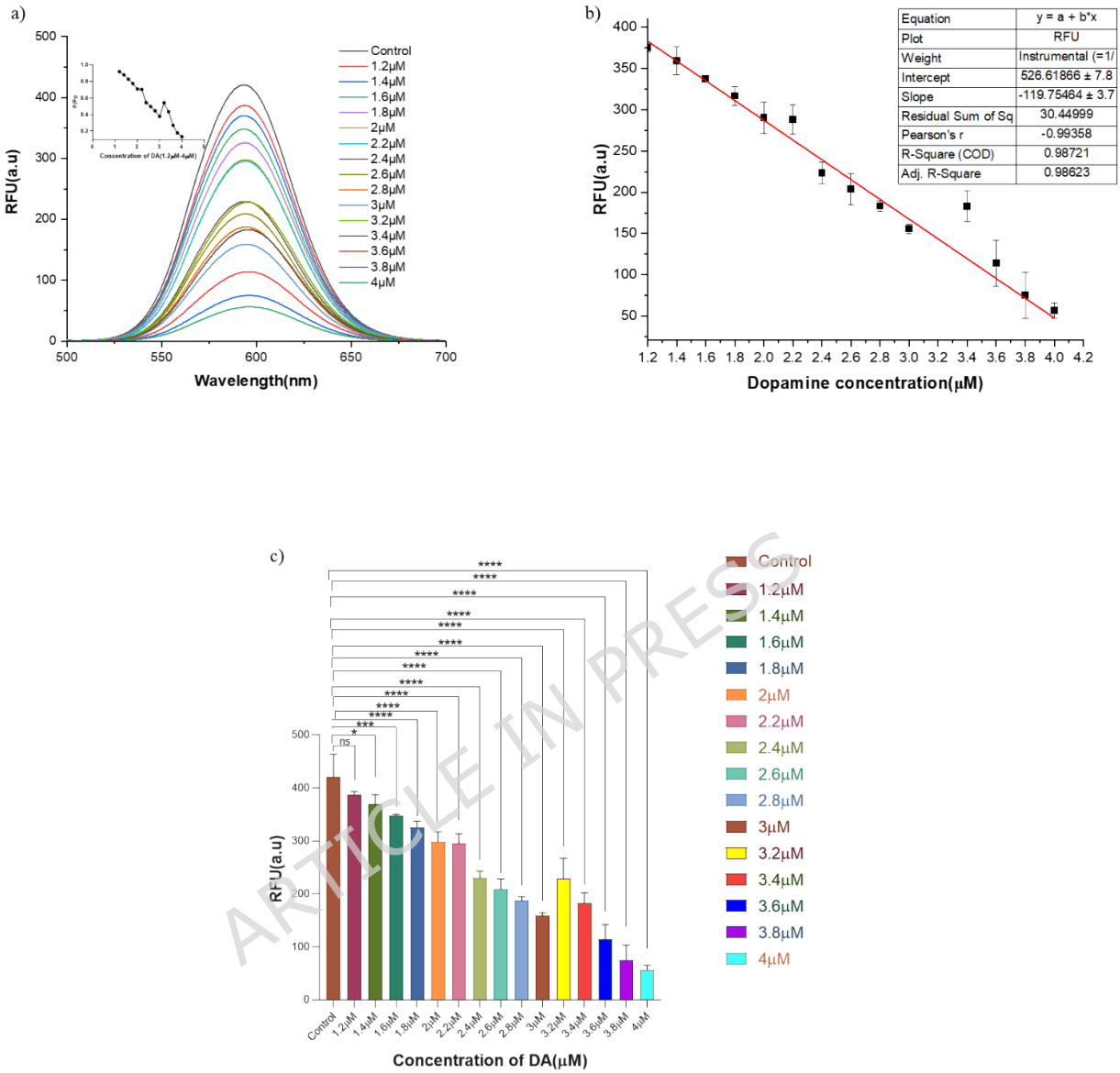

Fig.2: DA kinetics in an aqueous system

a) Fluorescence emission spectra of CdTe QDs in the presence of varying concentrations of DA, from 1.2 µM to 4 µM, at a fixed H_2O_2 (300 µM) and HRP (6 U). Control represents QD, H_2O_2, and HRP with no DA in PB. Increasing the concentration of dopamine results in enhanced fluorescence quenching until it reaches saturation.

b) DA standard deviation graph showing concentration-dependent fluorescence quenching from 1.2 µM to 4 µM with a fixed H_2O_2 (300 µM) and HRP (6 U), having an R^2=0.99

c) Bar graph indicating fluorescence intensity (RFU) measured in an aqueous system with increasing concentrations of dopamine (1.2 µM to 4 µM). A gradual decrease in fluorescence

intensity is observed with increasing dopamine concentration, indicating effective quenching by DA. Data were represented as mean ± SD (n = 3). Statistical analysis was performed using one-way ANOVA, followed by Dunnett's multiple-comparison test against the control group, with statistical significance ($p < 0.05$) relative to the control.

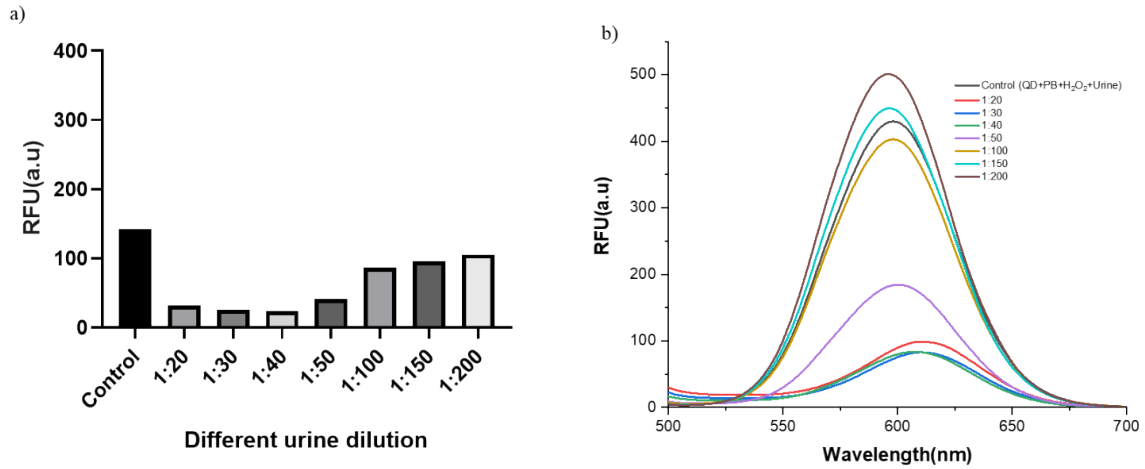

Fig.3: Fluorescence of CdTe QD-based dopamine biosensor in different dilutions of urine sample, ranging from 1:20,1:30,1:40,1:50,1:100,1:150, and 1:200 against a control having QD and PB (a), which was compared against a control having QD, PB, H_2O_2, and (1:100) urine. HRP

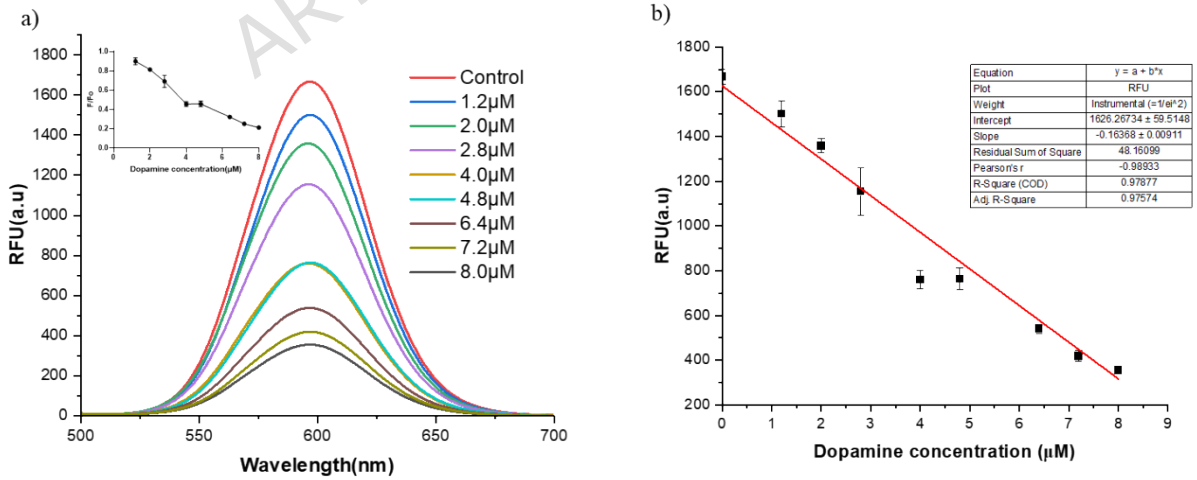

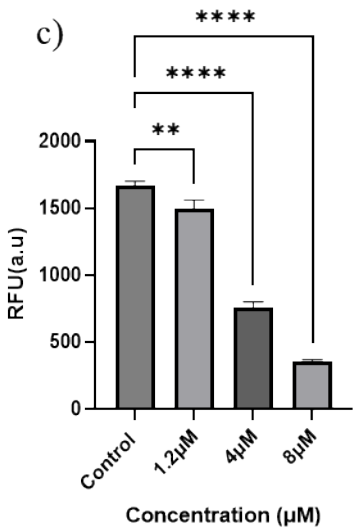

Fig.4: DA biosensing in urine

a) Fluorescence emission spectra of CdTe quantum dots-based DA biosensor in spiked urine samples, with DA concentration varying from 1.2 to 8 µM at a fixed H_2O_2 (300 µM) and HRP concentration (6 U). A progressive quenching of fluorescence with increasing DA concentration is observed due to the oxidation of DA and subsequent interaction with the CdTe QDs. The DA standard deviation graph shows concentration-dependent fluorescence quenching from 1.2 µM to 8 µM with fixed H_2O_2 (300 µM) and HRP (6 U), with R^2 = 0.97.

b) The DA standard deviation graph shows concentration-dependent fluorescence quenching from 1.2 µM to 8 µM with a fixed H_2O_2 (300 µM) and HRP (6 U), with an R^2=0.97

c) Bar graph indicating the detection of DA in spiked urine samples. The bar graph shows fluorescence intensity (RFU) measured after treating urine samples spiked with increasing concentrations of DA (1.2 µM to 8 µM). A gradual decrease in fluorescence intensity with increasing DA concentration indicates effective quenching. Data are represented as mean ± SD (n = 3). Statistical analysis was performed using one-way ANOVA, followed by Dunnett's multiple-comparison test against the control group, with statistical significance ($p < 0.05$) relative to the control.

Table 1: DA detection in urine and recovery percentage

Dopamine concentration (nM)	% Recovery
1200 nM	98.62%
2800 nM	96.81%
4000 nM	98.21%
7200 nM	94.25%

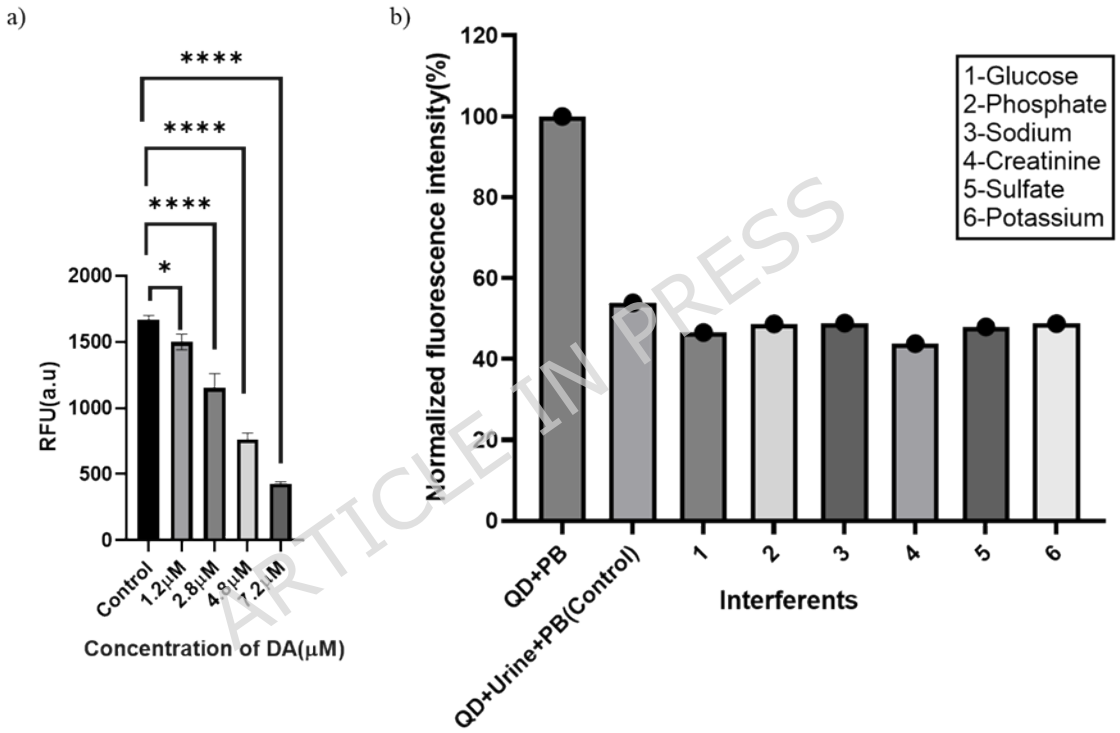

Fig.5:a) Spike and recovery of DA and (b) Interference of organic and inorganic constituents in the Urine sample.

a) Bar graph indicating detection and recovery with different DA concentrations (1.2 µM-7.2 µM). Data represent mean ± SD of three independent replicates (n = 3). Statistical analysis was performed using one-way ANOVA, followed by Dunnett's multiple comparisons test against the control group, with statistical significance ($p < 0.05$) compared to the control.

b) The interference of organic constituents such as Glucose (416.29 µM) and creatinine (70.72 µM), and inorganic constituents such as phosphate (0.03 µM), sodium (0.1 µM), sulphate (0.03 µM), and potassium (0.125 µM) in the urine sample was checked at a fixed H_2O_2 (300 µM) and HRP concentration (6 U).

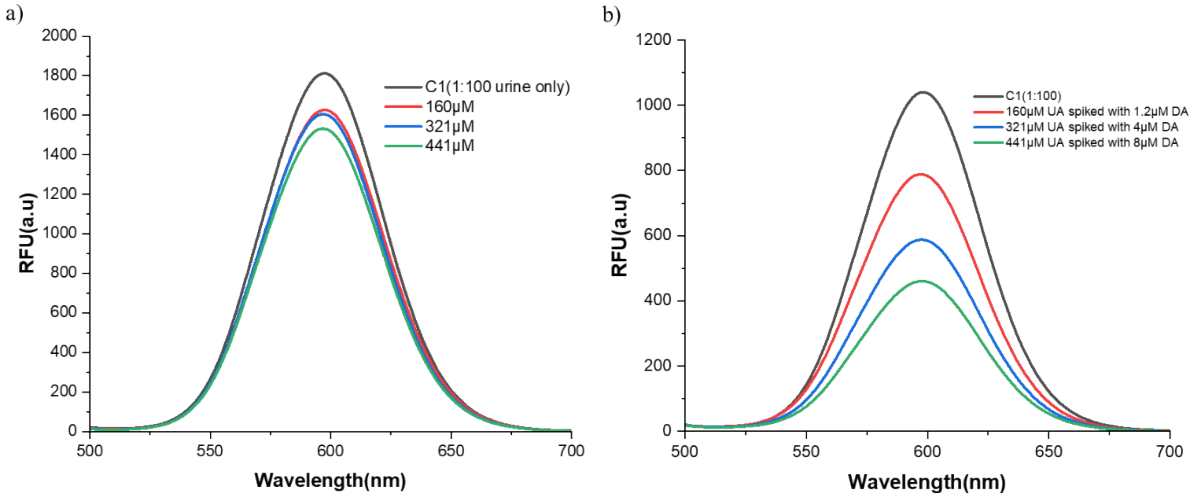

Fig.6: a) UA kinetics in urine and (b)DA interference with Uric acid in a urine sample.

Fluorescence emission spectra of CdTe quantum dots-based DA biosensor for different UA concentrations spiked to urine samples, with UA concentration varying from 160 μM, 321 μM, and 441 μM (a) and for different DA concentrations spiked to UA in urine samples, with DA concentration varying from 1.2 μM, 4 μM, and 8 μM, were spiked to UA of concentrations varying from 160 μM, 321 μM, and 441 μM at a fixed H_2O_2 (300 μM) and HRP concentration (6 U).